Plant Physiology, February 2000, Vol. 122, pp. 573–582, www.plantphysiol.org © 2000 American Society of Plant Physiologists

Nitric Oxide Modulates the Activity of Tobacco Aconitase[1]

Duroy A. Navarre, David Wendehenne[2], Jörg Durner[3], Robert Noad, and Daniel F. Klessig*

Waksman Institute and Department of Molecular Biology and Biochemistry, Rutgers, the State University of New Jersey, 190 Frelinghuysen Road, Piscataway, New Jersey 08854–8020

Recent evidence suggests an important role for nitric oxide (NO) signaling in plant-pathogen interactions. Additional elucidation of the role of NO in plants will require identification of NO targets. Since aconitases are major NO targets in animals, we examined the effect of NO on tobacco (*Nicotiana tabacum*) aconitase. The tobacco aconitases, like their animal counterparts, were inhibited by NO donors. The cytosolic aconitase in animals, in addition to being a key redox and NO sensor, is converted by NO into an mRNA binding protein (IRP, or iron-regulatory protein) that regulates iron homeostasis. A tobacco cytosolic aconitase gene (*NtACO1*) whose deduced amino acid sequence shared 61% identity and 76% similarity with the human IRP-1 was cloned. Furthermore, residues involved in mRNA binding by IRP-1 were conserved in NtACO1. These results reveal additional similarities between the NO signaling mechanisms used by plants and animals.

Over the last decade, extensive research about the role of nitric oxide (NO) in animals has demonstrated that it is a key signal molecule involved in a wide variety of processes including vasorelaxation, neurotransmission, and the innate immune response (Schmidt and Walter, 1994). In contrast, the role of NO in plants is less well understood. Recently, two reports showed that NO is a signal molecule in plant defense responses (Delledonne et al., 1998; Durner et al., 1998). NO was found to be essential for the full activation of plant disease resistance and programmed cell death in soybean and Arabidopsis (Delledonne et al., 1998). In addition, tobacco (*Nicotiana tabacum*) plants mounting a successful resistance response to tobacco mosaic virus (TMV) exhibited increased nitric oxide synthase (NOS)-like activity, whereas susceptible infected plants did not (Durner et al., 1998). Furthermore, exogenous NO induced expression of the genes encoding two commonly used plant defense markers, Phe ammonia lyase (PAL) and the pathogenesis-related (PR)-1 protein.

The second messenger, cyclic GMP (cGMP), which is synthesized following the activation of guanylate cyclase by NO, mediates many NO responses in animals (Schmidt and Walter, 1994; Stamler, 1994). cGMP also appears to function as a NO second messenger in tobacco, because exogenous NO treatment resulted in a transient increase in cGMP levels (Durner et al., 1998). Furthermore, exogenous cGMP induced *PAL* expression, while guanylate cyclase inhibitors suppressed NO-mediated activation of *PAL*. cADP Rib, which sometimes acts downstream of cGMP in the animal NO signaling pathway, was also shown to induce *PAL* and *PR-1* expression in tobacco (Durner et al., 1998). These results suggest the presence of a functional NO signaling system in the tobacco defense response that has considerable conservation with NO signaling pathways of animals.

Although many NO-mediated effects in animals are cGMP dependent, NO can also function in a cGMP-independent manner through mechanisms including S-nitrosylation of thiol-containing proteins and Tyr nitration, or via the direct interaction of NO with metal-containing proteins (Kroncke et al., 1997; Ischiropoulos, 1998). NO is able to readily interact with proteins because of its small size and lack of charge, features that give it access to the interior of proteins. Furthermore, NO has a half-life of 5 to 15 s and is readily diffusible in both aqueous and lipid environments, properties that facilitate its function as a signal molecule (Fukuto, 1995; Nathan, 1995; Lancaster, 1997).

Despite the well-described effects of NO on many physiological processes in animals, the direct targets of NO or its second messengers are less well characterized (Hausladen and Stamler, 1998). In addition to guanylate cyclase, aconitases are a major NO target in animals (Drapier, 1997; Mott et al., 1997), and NO directly affects aconitase functionality (Gardner et al., 1997). Aconitase is an iron-sulfur (4Fe-4S)-containing enzyme that catalyzes the reversible isomerization of citrate to isocitrate. It has two isoforms, one located in mitochondria and the other in the cytosol. In animals, NO reversibly inactivates both aconitases by promoting the loss of the iron-sulfur cluster, which can subsequently be reassembled under the proper conditions (Drapier, 1997). The mitochondrial aconitase is a constituent of the Krebs cycle, so its inactivation by NO decreases cellular energy metabolism. This inactivation of aconitase may have a protective effect against additional oxidative stress by acting as a reversible "circuit breaker" (Gardner and Fridovich, 1991). Inactivation results in reduced electron flow through the mitochondrial electron transport chain, and thereby decreases the generation of reactive oxygen species (ROS), the natural by-products of respiration. Conversely, aconitase inactivation has been proposed

[1] This work was supported by the National Science Foundation (grant nos. MCB 9723952 and MCB 9514239).

[2] Present address: Unité associée Institut National de la Recherche Agronomique/Université de Bourgogne, Institut National de la Recherche Agronomique AV 1540, 21034 Dijon cedex, France.

[3] Present address: Institute of Biochemical Plant Pathology, GSF-National Research Center for Environment & Health, D–85764, Oberschleissheim, Germany.

* Corresponding author; e-mail klessig@waksman.rutgers.edu; fax 732–445–5735.

to increase ROS generation due to the accumulation of reduced metabolites, a condition termed "reductive stress" (Yan et al., 1997).

Aconitase is exquisitely sensitive to ROS and is more vulnerable than other iron-sulfur- or heme-containing enzymes to inhibition by NO (Castro et al., 1994) and other ROS (Verniquet et al., 1991). If the tobacco aconitases, like their animal counterparts, are inhibited by NO and other ROS, this could be significant during host-pathogen interactions in which both NO and other ROS are produced (Alvarez and Lamb, 1997; Doke, 1997; Delledonne et al., 1998; Durner et al., 1998). One example of the biological consequences of the lability of aconitase to ROS is seen in houseflies, in which a selective oxidative inactivation of aconitase is thought to be responsible for some of the physiological effects of aging (Yan et al., 1997).

An unexpected additional role for aconitase in animals was found when the iron-regulatory protein (IRP), a protein that controls iron homeostasis, was determined to be the cytosolic isoform of aconitase (Kaptain et al., 1991; Klausner et al., 1993). IRP binds mRNAs containing a specific iron-responsive element (IRE) consensus sequence and thereby regulates their translatability and/or stability. This mRNA-binding activity has been detected in vertebrates, annelids, and insects, but not in yeast, bacteria, or plants (Hentze and Kuhn, 1996). However, recently, the *Bacillus subtilis* aconitase was shown to bind IREs (Alen and Sonenshein, 1999). IREs have been identified in a variety of mRNAs, including those for genes encoding ferritin, aminolevulinic acid synthase, and the transferrin receptor (Domachowske, 1997). The binding of IRP to IREs located in the 5′ region of the transcript (e.g. ferritin, aminolevulinic acid synthase) prevents translation, whereas binding to those in the 3′ region improves transcript stability (e.g. transferrin receptor). NO converts the cytosolic aconitase into an IRP by promoting the loss of the iron-sulfur cluster, which otherwise prevents IRE binding. Consequently, the activities of aconitase and IRP are mutually exclusive and are regulated in part by NO. Thus, aconitase, in addition to being a key NO sensor in animals, also regulates iron homeostasis.

Given the similarities in NO signaling between plants and animals, we examined whether NO affects tobacco aconitases. In this paper we show further similarities between NO signaling in plants and animals. We found that NO inhibits aconitase. The possible significance of NO-mediated aconitase inhibition during plant-pathogen interactions and parallels between NO signaling in plants and animals is discussed.

MATERIALS AND METHODS

Plant Material and Growth Conditions

Tobacco (*Nicotiana tabacum* cv Xanthi nc [NN]) plants were grown in growth chambers at 22°C with a 14-h light cycle. Plants 6 to 10 weeks old were used for TMV infection and chemical treatments. Greenhouse-grown plants 4 to 5 weeks old were used for the purification of aconitase. Infections with TMV strain U1 and temperature shift experiments were conducted as previously described (Malamy et al., 1992).

Aconitase Assay

Extracts containing aconitase activity were prepared from 15 g of young tobacco leaves that were homogenized in 45 mL of extraction buffer (25 mM imidazole, 1 mM EDTA, 2 mM $MgCl_2$, 40 mM KCl, 0.1% [w/v] bovine serum albumin, 1% [w/v] insoluble polyvinyl-polypyrrolidone [PVPP, Sigma-Aldrich, St. Louis], 2 mM dithiothreitol [DTT], 2 mM citrate, 1 mM phenylmethylsulfonyl fluoride (PMSF), and 10% [v/v] glycerol; pH 7.4). Extracts were desalted on a PD-10 column (Pharmacia Biotech, Piscataway, NJ) equilibrated with aconitase buffer (20 mM imidazole, pH 7.5, 2 mM citrate, 1 mM DTT, 1 mM EDTA, and 10% [v/v] glycerol) and concentrated in a Centricon-10 column (Millipore, Bedford, MA). Extracts were treated with freshly prepared 6-(2-hydroxy-1-methyl-2-nitrosohydrazino)-*N*-methyl-1-hexanimine (NOC-9) or 3-morpholinosydnonimine-HCl (SIN-1) (Calbiochem or Alexis, San Diego) as described in the text, and then passed through a Sephadex G-25 spin column to remove the NOC-9 or SIN-1 prior to measuring activity. Aconitase activity was measured at room temperature in 75 mM Tris-HCl (pH 8.0) by following the formation of cis-aconitate from isocitrate at 240 nm (Kennedy et al., 1983). All aconitase inhibition experiments were repeated at least three times with two replications for each point. The data for one representative experiment are shown. Reactivation of tobacco aconitase was attempted using 1 to 10 mM DTT or Cys and 0.1 to 0.5 mM ferrous ammonium sulfate. Fumarase was assayed by measuring the change in absorbance at 240 nM as described by Hill and Bradshaw (1969).

Purification of Tobacco Aconitase

Approximately 600 g of leaves was homogenized in a blender with 4 volumes of extraction buffer (50 mM imidazole, pH 7.5, 2 mM citrate, 2 mM ascorbate, 2 mM DTT, 1 mM PMSF, and 1% [w/v] polyvinylpyrrolodine), and centrifuged at 15,000*g* for 10 min at 4°C. A 45% to 75% $(NH_4)_2SO_4$ fraction was collected from this supernant and applied to a Sephadex G-100 column (30 × 450 mm) equilibrated with 20 mM imidazole, pH 7.5, 2 mM citrate, 1 mM DTT, 1 mM EDTA, 150 mM $(NH_4)_2SO_4$, and 10% (v/v) glycerol. Active fractions were collected, pooled, and adjusted to 1.25 M $(NH_4)_2SO_4$. Subsequent chromatography used an automated FPLC system (Pharmacia Biotech). The sample was applied to a phenyl-sepharose column (XK 16/20, Pharmacia Biotech) equilibrated with 20 mM imidazole, pH 7.5, 1.25 M $(NH_4)_2SO_4$, 2 mM citrate, 1 mM EDTA, 1 mM DTT, and 10% (v/v) glycerol, and eluted with a decreasing linear gradient of $(NH_4)_2SO_4$ (1.25–0 M). Active fractions were pooled and desalted on PD-10 columns equilibrated with aconitase buffer. The sample was applied to a HiTrap Q-Sepharose column (5×5, Pharmacia Biotech) and eluted with a linear increasing gradient of NaCl (0–300 mM) in aconitase buffer. Fractions showing the highest activity were pooled and desalted. Desalted samples were

applied to a Mono-Q column (5/5, Pharmacia Biotech) and eluted with an increasing NaCl gradient (0–300 mM) in aconitase buffer. Fractions with the highest specific activity were again pooled and concentrated using a Centricon-10 cartridge. The sample was loaded onto a Superdex-200 HR column (10/30, Pharmacia Biotech) equilibrated with aconitase buffer and eluted in the same buffer using a flow rate of 0.75 mL/min. Partially purified aconitase was stable for at least 1 month when stored at −80°C under N_2, without multiple freeze-thaw cycles. The protein concentration was determined using the Bradford assay (Bio-Rad Laboratories, Hercules, CA) with bovine serum albumin as the standard.

Distribution of Aconitase

The amount of mitochondrial versus cytosolic aconitase was determined by gently homogenizing leaves in 4 volumes of an osmotic buffer containing 330 mM sorbitol, 30 mM 3-(N-morpholino)-propanesulfonic acid (MOPS), pH 7.5, 2 mM ascorbate, 2 mM citrate, 2 mM malate, 5 mM β-mercaptoethanol, 1 mM EDTA, and 1.5% (v/v) insoluble PVPP. All work was done at 4°C. Extracts were centrifuged at 18,000*g* for 15 min and separated into a supernatant and a pellet fraction. The supernatant was considered the "cytosolic" fraction, while the pellet was considered the organellar fraction. The pellet was lysed by vortexing in a non-osmotic buffer (buffer A) containing 20 mM imidazole, pH 7.5, 1 mM EDTA, 1 mM citrate, 1 mM malate, 1 mM DTT, and 10% (v/v) glycerol. Both the lysed organellar fraction and the "cytosolic" fraction were adjusted to 35% saturation with $(NH_4)_2SO_4$ and centrifuged for 10 min at 18,000*g*. The supernatant from each fraction was collected and adjusted to 75% saturation with $(NH_4)_2SO_4$. The resulting precipitate was collected by centrifugation for 10 min at 18,000*g*. The pellets were resuspended in equal volumes of buffer A and assayed for aconitase and fumarase activity.

Isolation and Sequencing of the Tobacco Cytoplasmic Aconitase cDNA

PCR was used to amplify cytoplasmic aconitase cDNAs from a λ-ZAP tobacco cDNA library. The library was constructed from RNA extracted from tobacco leaves infected with TMV (Guo et al., 1998). The degenerate oligonucleotide primers used were (5′–3′) TCYTCYATGGCYKCXGARAAYCC (primer 5′) and ACYGCYGGYACYCCXGTRAARTC (primer 3′) (K = G + T, R = G + A, Y = T + C, X = A + C + G + T). These primers correspond to conserved regions between Arabidopsis and human cytoplasmic aconitase. PCR was carried out in 50 μL of volume containing 50 mM KCl, 10 mM Tris-HCl, pH 8.3, 2.5 mM $MgCl_2$, 200 μM each dNTP, and 2.5 units of *Taq* polymerase (Amplitaq, Perkin-Elmer Applied Biosystems, Foster City, CA) with 150 ng of phage library template DNA and 50 pmol of each of the primers. PCR was conducted using an initial template denaturation step of 5 min at 94°C, followed by 30 cycles of 30 s at 94°C, 1 min at 55°C, and 1 min at 72°C. After the 30th cycle, an elongation step of 5 min at 72°C was used.

PCR fragments of the expected size (300 bp) were cloned into a pSK^+ vector and sequenced using the Sequenase Version 2.0 sequencing kit (Amersham-Pharmacia Biotech, Uppsala, Sweden). A PCR fragment with homology to cytoplasmic aconitase was then used to screen a λ-ZAP cDNA library from tobacco leaves to recover a full-length clone. Library screening used Hybond-N filters (Amersham-Pharmacia Biotech) and hybridization was conducted according to the method of Sambrook et al. (1989). Plaques that hybridized to the probe were purified and in vivo excision was used to obtain pBK-CMV phagemid (Stratagene, La Jolla, CA). The sequence of the full-length clone was determined either by making appropriate subclones in pUC19 vectors or by primer walking. The DNA sequence was determined in both directions by using the Sequenase Version 2.0 sequencing kit (Amersham-Pharmacia Biotech) and the Robert Wood Johnson Medical School Sequencing Lab (University of Medicine and Dentistry of New Jersey, Rutgers University, Piscataway).

Overexpression and Purification of the Recombinant Aconitase

The putative tobacco cytoplasmic aconitase cDNA (*NtAco1*) was subcloned into a *Sac*I site in a pET28a plasmid vector (Novagen, Madison, WI) under the control of the T7 bacteriophage promoter. Expression of the recombinant *NtACO1* in *Escherichia coli* strain BL21(DE3) was induced by addition of isopropyl-β-D-thiogalactopyranoside concentrations ranging from 100 μM to 0.5 mM at temperatures from 20°C to 37°C. Extraction of the recombinant aconitase and purification on a nickel column was performed according to the manufacturer's instructions (Novagen). The size of the recombinant aconitase containing a His- and a T7-tag was approximately 113 kD on an 8% SDS-polyacrylamide gel.

Analysis of *NtACO1* Expression

Expression of *NtACO1* was examined in response to various chemicals, including NO donors (0.5 mM SNAP, 0.5 mM GSNO, and 0.5 mM SIN-1), 10 mM H_2O_2, and 0.5 mM salicylic acid (SA). Leaves were injected with the various chemicals, after which leaf discs were collected over intervals ranging from 0 to 24 h post injection. Total RNA was extracted from leaf discs using the TRIZOL reagent according to the manufacturer's instructions (Life Technologies/Gibco-BRL, Cleveland). For reverse transcriptase (RT)-PCR, total RNA prepared as described above was treated with amplification grade deoxyribonuclease 1 (Life Technologies/Gibco-BRL) and then subjected to cDNA synthesis using RT(Superscript II, Life Technologies/Gibco-BRL). First-strand synthesis was carried out using a 14-mer oligo-dT primer. Primers to *NtACO1* and β-tubulin were designed based on the sequence of the actual tobacco genes, and were predicted to generate PCR products of 476 and 373 bp, respectively.

The correct identity of the PCR products was confirmed by both the expected fragment size and by the use of aconitase and β-tubulin cDNAs to probe gel blots contain-

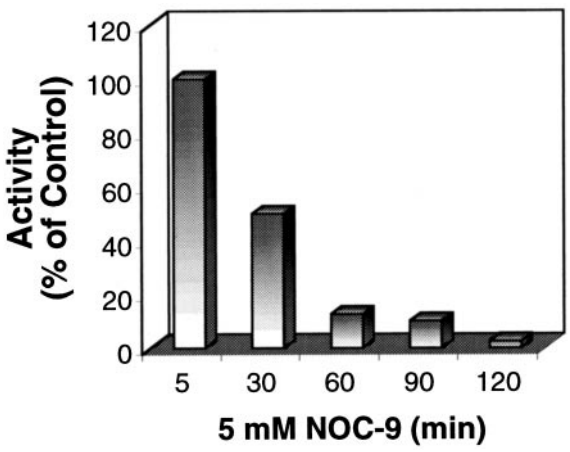

Figure 1. Inhibition of aconitase in leaf extracts treated with NOC-9. Tobacco leaf extracts were incubated with 5 mM NOC-9 on ice for the times indicated. Results are expressed as the percentage of control samples incubated without NOC-9 for the same times.

ing the RT-PCR products. PCR reactions used a 2-min denaturation at 94°C, followed by 21 to 25 cycles of 30 s at 94°C, 30 s at 56°C, and 30 s at 72°C, and a single elongation step of 5 min at 72°C. β-Tubulin was used as an internal control. Identical volumes of each reaction were loaded into an agarose gel and the amount of aconitase transcript in each sample was judged relative to the amount of β-tubulin in the same sample. Visualization of bands was achieved initially using radiolabeling, phosphor imaging (Molecular Dynamics, Sunnyvale, CA) analysis, and ethidium bromide staining. No significant differences were observed between the two detection techniques, so ethidium bromide staining was used routinely.

RESULTS

NO Inhibits Aconitase Activity in Tobacco Crude Extracts

Mammalian aconitases are a major direct NO target (Drapier, 1997). As a first step toward determining whether plant aconitases are also regulated by NO, a crude cellular extract containing an aconitase activity of 3 to 8 units/mg protein was prepared from tobacco leaves. In the presence of citrate, activity was stable at 4°C for several hours. These extracts were able to utilize both citrate and isocitrate as substrates in an aconitase assay. Furthermore, the aconitase inhibitor fluorocitrate inhibited activity. Extracts were treated with the NO donor NOC-9 for various times as shown in Figure 1. Treatment with 5 mM NOC-9 for 30 min reduced activity approximately 50% relative to the mock-treated control and by 1-h inhibition was approximately 90%.

Partial Purification of Tobacco Aconitase

While we could demonstrate NO-mediated inhibition of aconitase in leaf extracts (Fig. 1), the extracts likely contained many non-specific scavengers that titrate out the available NO and other ROS. For example, very high concentrations of H_2O_2 (5–10 mM), a potent inhibitor of aconitase, were needed to give significant inhibition (data not shown). This poor sensitivity to H_2O_2 was probably due to the presence of catalases and peroxidases in the crude extracts. Furthermore, NOC-9 concentrations below 5 mM had little effect on aconitase activity. To overcome these limitations, we partially purified aconitase from tobacco leaves approximately 165-fold (Table I). Total aconitase was purified and activity was present as a single broad peak. Separate peaks of activity attributable to the mitochondrial and cytosolic isoforms were not observed. Analysis of the pooled fractions from each purification step by SDS-PAGE revealed a significant enrichment of the putative aconitase during a six-step process (Fig. 2). This corresponds to the reported purification of aconitase from potato (130-fold, Verniquet et al., 1991), pumpkin (100-fold, De Bellis et al., 1993), and melon (870-fold, Peyret et al., 1995).

Tobacco aconitase was increasingly unstable with progressive purification, which is consistent with its known lability in aerobic conditions. Mammalian aconitases also lose activity during purification, but are readily reactivated in the presence of iron and a reducing agent (Kennedy et al., 1983). In contrast, we were unable to reactivate the tobacco aconitase once activity declined or was completely lost. Commercially available pig aconitase, however, was readily reactivated. Other groups have also been unable to reactivate plant aconitases (Brouquisse et al., 1987; Verniquet et al., 1991; De Bellis et al., 1993). This inability to be reactivated likely contributes to the low yields and modest purification reported in the literature.

Table I. *Purification of aconitase*

Partial purification of aconitase from 600 g of tobacco leaves.

Fraction	Total Protein	Total Activity	Specific Activity	Purification	Yield
	mg	*units*	*units mg^{-1}*	*fold*	*%*
Total extract	6,076	25,521	4.2	–	–
45%–75% $(NH_4)_2SO_4$	504	40,522	80	19	158
Sephadex G100	306	34,605	113	27	136
Phenyl-Sepharose	63	15,498	246	59	61
Q-Sepharose	8	3,204	401	95	13
Mono-Q	1.5	945	630	150	3.7
Superdex 200	0.4	280	700	167	1.1

Inhibition of Partially Purified Aconitase

The ability of NO to inhibit the activity of partially purified aconitase was tested by treatment with different concentrations of NOC-9 for 15 min at 37°C. Figure 3A shows that 1 or 5 mM NOC-9 completely inhibited aconitase activity, while 0.5 mM NOC-9 caused approximately 50% inhibition. Aconitase activity was also inhibited when treated for 1 h at 37°C with SIN-1 (Fig. 3B). SIN-1 releases NO and superoxide, which react rapidly to produce peroxynitrite ($ONOO^-$). Greater than 50% and 80% inhibition was achieved by 0.5 mM and 5 mM SIN-1, respectively, and inhibitory effects were observed with as low as 0.1 mM SIN-1 (Fig. 3B). Millimolar concentrations of SIN-1 and NO donors in general are thought to liberate micromolar concentrations of NO (Bouton et al., 1997; Melino et al., 1997). Inhibition of animal aconitases by SIN-1 concentrations of 1 to 30 mM have been reported, and a 2-h incubation with 2 mM SIN-1 gave 80% inhibition. (Bouton, et al., 1997; Grune, et al., 1998). Thus, tobacco and mammalian aconitases appear to share a similar sensitivity to NO and its derivatives.

Aconitase is also known to be inhibited by other ROS (Verniquet et al., 1991; Gardner et al., 1995). Therefore, the effect of H_2O_2 on the partially purified tobacco aconitase was tested (Fig. 3C). Treatment for 1 h at 4°C with as little as 25 μM H_2O_2 dramatically reduced aconitase activity; even as little as 100 nM H_2O_2 resulted in significant inhibition. This is in contrast to the high levels of H_2O_2 (5–10 mM) needed to inhibit aconitase in crude leaf extracts. Moreover, when aconitase was treated with 100 μM or more H_2O_2, a nearly instantaneous inhibition of 50% or greater occurred (data not shown). In animals, H_2O_2 and NO appear to activate IRP-1 in vivo by distinct mechanisms, with H_2O_2 activating IRP-1 within 60 min of treatment, whereas NO requires up to 15 h (Pantopoulos and Hentze, 1995; Hentze and Kuhn, 1996).

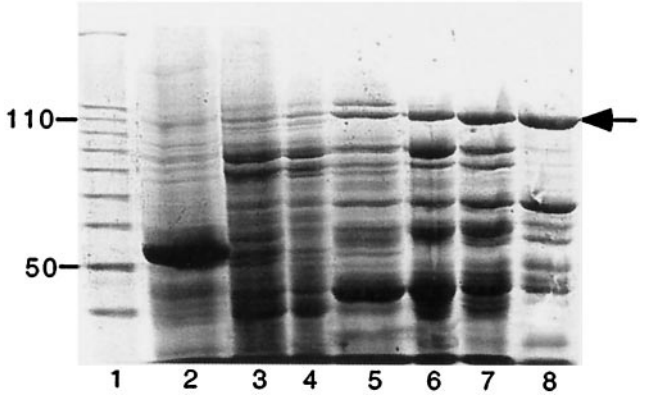

Figure 2. SDS-PAGE analysis of tobacco aconitase purification. An aliquot of protein sample from each purification step was analyzed by 8% acrylamide SDS-PAGE. The Coomassie blue-stained gel is shown. Lane 1, 10-kD protein ladder; lane 2, total extract; lane 3, 45% to 75% $(NH_4)_2SO_4$ fraction; lane 4, pooled fractions from the Sephadex G100 column; lane 5, pooled fractions from the phenyl-sepharose column; lane 6, pooled fractions from the Q-sepharose column; lane 7, pooled fractions from the Mono-Q column; lane 8, pooled fractions from the Sephadex 200 HR column. The 50- and 110-kD proteins of a 10-kD protein marker ladder are indicated on the left. The position of the putative aconitase is denoted by an arrow at the right.

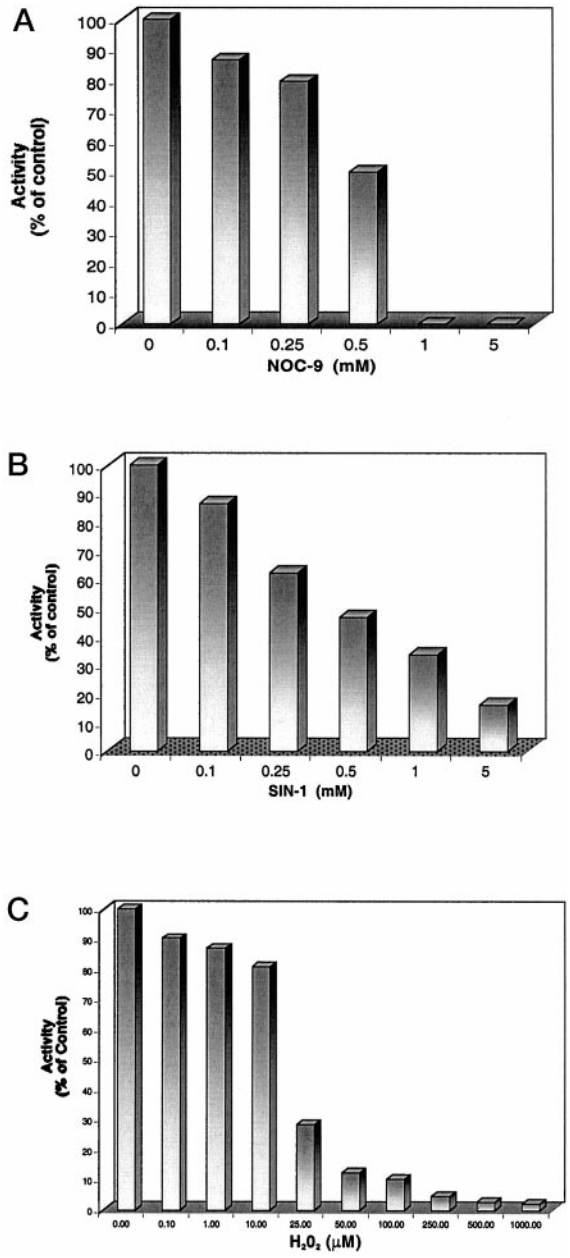

Figure 3. Inhibition of partially purified aconitase by NOC-9, SIN-1, and H_2O_2. Partially purified aconitase from tobacco leaves, prepared as described in Table I, was used for aconitase assays. A, Samples were incubated for 15 min at 37°C with the indicated amounts of NOC-9. Results are expressed as a percentage of a buffer-treated control. B, Samples were incubated with the indicated amounts of SIN-1 for 1 h at 37°C. Results are expressed as a percentage of a buffer-treated control. C, Samples were incubated with the indicated amounts of H_2O_2 for 1 h at 4°C. Results are expressed as a percentage of a buffer-treated control.

Aconitase in plants is found only in mitochondria and in the cytosol, where it participates in the glyoxylate cycle (Brouquisse et al., 1987; Courtois-Verniquet and Douce,

Figure 4. Comparison of the deduced amino acid sequence of NtACO1 with the human IRP-1. Colons represent amino acids that are identical between IRP-1 and NtACO1, plus signs represent conserved amino acid differences, and dashes represents gaps introduced to maximize alignment. The underlined, bolded amino acids are involved in mRNA binding in animal IRPs.

```
NtACO1 MAAENPFKGILTVLPKPGGGEFGKYYSLPALNDPRIDKLPYSSRILLESAIRNCDNFQVK 60
IRP-1  :S--:::AH+AEP:DPVQP:+--:+++:NK:E:S:YG+:::+:I:+:::+::::::E:L::

NtACO1 KEDVEKIIDWENTAPKLVEIPFKPARVLLQDFTGVPAVVDLACMRDAMNKLGSDSDKINP 120
IRP-1  :+:+:N:+H:NV:QH:N+:+:::::::+:::::::::::::F:A::::+K:::G:P+::::

NtACO1 LVPVDLVIDHSVQVDVARSENAVQANMELEFQRNKERFAFLKWGSNAFHNMLVVPPGSGI 180
IRP-1  +C:A:::::::+:::FN:RA+++:K:Q+:::+:::+:::E::::::Q:::::R++:::::::

NtACO1 VHQVNLEYLGRVVFNREGLLYPDSVVGTDSHTTMIDGLGVAGWGVGGIEAEATMLGQPMS 240
IRP-1  +:::::::::A:::+++:GG::::+:::::::::::::::+L:::::::::::V::::::+:

NtACO1 MVLPGVVGFKLSGKLRSGVTATDLVLTVTQMLRKHGVVGKFVEFYGDGMSELSLADRATI 300
IRP-1  :::::Q:+:++:M::PHPL::+::+::::+:+H::+V:::::::::::+:P:+++::+:::::

NtACO1 ANMSPEYGATMGFFPVDHVTLQYLKLTGRSDETVEMIEAYLRANKMFVDYDEPQHEKVYS 360
IRP-1  :::C:::::::AA:::::E:++T::VQ::::D+:K++Y:+K::+:VG::R:+++:SQ+PD++

NtACO1 SCLHLDLAGVEPCVSGPKRPHDRVPLKEMKSDWHSCLDNKVGFKGFAVPKDAQEKVVKFS 420
IRP-1  QV+E:::KT:V::C:::::::Q:+:A+S+::K:+E:::GA:Q:::::Q:AP+HHNDHKT:I

NtACO1 FHGQDAELKHGSVVIAAITSCTNTSNPSVMLGAALVAKKACDLGLHIKPWVKTSLAPGSG 480
IRP-1  +DNT+FT:A:::::::::::::::::::::::::::::G:+::::V:A::++M:++:::+::::

NtACO1 VVTKYLLQSGLQKYLNQQGFHIVGYGCTTCIGNSGDLDESVASAISENDIVAAAVLSGNR 540
IRP-1  :::Y::Q+:::+MP::::+:L::D+:::::M:::::::P:P:P:VE::++G:+::VG:::::::

NtACO1 NFEGRVHPLTRANYLASPPLVVAYALAGTVDIDFEKEPIGVGNDGKNVYFKDIWPSTEEI 600
IRP-1  ::::::::N:::::::::::::+:::+::+R:::::::+:::NAK:+Q:+L:::::+R+::

NtACO1 AEVVQSSVLPDMFKSTYEAITKGNNMWNQLSVPSSKLYSWDTSSTYIHEPPYFKDMTMDP 660
IRP-1  QA:E+QY:+:G:::EV:+K:ETV:ES::A:+T::D::+F:++K::::KS::+:+++:+:L

NtACO1 PGPHGVKDAFCLLNFGDSITTDHISPAGSIHKDSPAAKYLTERGVDRRDFNSYGSRRGND 720
IRP-1  QP:KS+V::+V:::L:::+:::::::::+:A++:::+:::N::+TP:+::::::::::::

NtACO1 EIMARGTFANIRIVNKLLNGEVGPKTIHIPTGEKLSVFDAAMKYKSAGQDTIILAGAEYG 780
IRP-1  A+:::::::::::++:+F::K+ A:+:::+:+::I:D:::::E+:+Q::LPL:+:::K:::

NtACO1 SGSSRDWAAKGPMLLGVKAVIAKSFERIHRSNLVGMGIVPLCFKAGEDAETLGLTGHERY 840
IRP-1  +::::::::::::F:::+:::+:+:+::::::::::::::++::E+LP::+:+A:::::Q:::

NtACO1 TIDLPEKISEIHPGQDVTVRTDTGKSFTCIVRFDTEVELAYFNHGGILPYVIRQLIQQ  900
IRP-1  ::I+::N+K---:QMK:Q:+L::::+:QA++::::+:::T::L+::::N:+::++A+-
```

1993). The complete inhibition of aconitase activity by millimolar concentrations of NO donors suggested that NO inhibited both the tobacco cytosolic and mitochondrial aconitases. However, if the cytosolic isoform of aconitase represents only a small percentage of total activity, then the larger pool of inhibited mitochondrial aconitase could mask the resistance of the cytosolic aconitase. To resolve this question, the relative amount of cytosolic versus mitochondrial aconitase in tobacco leaves was determined by isolating a "cytosolic fraction" and a total organellar fraction containing the mitochondria. Fumarase, a commonly used mitochondrial marker enzyme, was used to determine the degree of mitochondrial contamination from lysed or leaky mitochondria in the cytosolic fraction.

Based on four independent experiments, approximately 75% (range approximately 55%–90%) of the total aconitase activity in tobacco leaves is cytosolic and the remaining approximately 25% mitochondrial. These results are consistent with those of other studies that estimated plant cytosolic aconitase comprises from 50% to greater than 90% of total activity (Courtois-Verniquet and Douce, 1993; De Bellis et al., 1995). Thus, given that 1 or 5 mM NOC-9 completely inhibited aconitase activity (Fig. 3A), we concluded that both the cytosolic and mitochondrial aconitases are sensitive to NO.

Cloning of a Tobacco Cytosolic Aconitase

NO has two distinct effects on mammalian aconitases: it inhibits the activity of both mitochondrial and cytosolic aconitases and also converts the cytosolic aconitase into IRP, a mRNA-binding protein. The results described above showed that the tobacco cytosolic aconitase is inhibited by NO, but do not address whether it can function as a mRNA-binding protein. As a first step to address this question, we cloned the tobacco cytosolic aconitase.

Cytosolic aconitase genes have been cloned from Arabidopsis (Peyret et al., 1995) and pumpkin (Hayashi et al., 1995). To obtain the corresponding tobacco gene, degenerate primers corresponding to sequences conserved between human and Arabidopsis cytosolic aconitases were used to generate a approximately 300-bp fragment, which was then used to screen a λ-ZAP cDNA library from tobacco leaves (Guo et al., 1998). A 3.1-kb cDNA clone was identified, sequenced, and found to contain a complete open reading frame encoding a protein of 898 amino acids with a predicted size of 98 kD and a pI of 6.1. The encoded protein had 91% identity and 95% similarity with the pumpkin cytosolic aconitase (Hayashi et al., 1995) and 85% identity and 91% similarity with the Arabidopsis cytosolic aconitase (Peyret et al., 1995). This cDNA was designated *NtACO1* and comparison with the human IRP-1 revealed 61% identity and 76% similarity as shown in Figure 4 (Kaptain et al., 1991). Interestingly, the putative tobacco cytosolic aconitase contains nine amino acid residues of a 10-residue sequence (DLVIDHSVQV) that in the human IRP-1 is believed to directly interact with IREs (Fig. 4; Basilion et al., 1994). Moreover, three Arg residues (540, 545, 785) involved in RNA binding by IRP-1 are also conserved (Fig. 4; Philpott et al., 1994).

NtACO1 was then subcloned into a pET28a vector, and the resulting His- and T7-tagged protein was overexpressed in *E. coli*. The recombinant protein accumulated in inclusion bodies and was examined for aconitase activity after solubilization and refolding. A low level of aconitase activity (2–4 units/mg protein) was detected after induction of the recombinant gene with isopropyl-β-D-thiogalactopyranoside and purification of the His-tagged protein, confirming that the putative cytosolic aconitase clone has aconitase activity. However, this activity could not be increased by either activating with reducing agents and Fe, by varying bacterial growth conditions, or by using

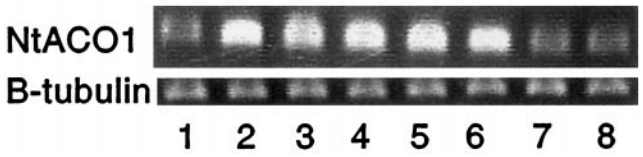

Figure 5. RT-PCR analysis of aconitase gene expression. Levels of *NtACO-1* and β-tubulin mRNA were measured by RT-PCR. cDNA prepared from total RNA by RT was amplified and the RT-PCR products electrophoresed in a 1.75% agarose gel. Gels were stained with ethidium bromide and photographed. β-Tubulin was used as a constitutively expressed control for each RT-PCR reaction. Lane 1, Leaf cDNA; lane 2, mature flower cDNA; lane 3, flower bud cDNA; lane 4, petal cDNA; lane 5, anther cDNA; lane 6, ovary cDNA; lane 7, cDNA from leaves treated 16 h with recombinant rat neuronal NOS plus cofactors and substrate; lane 8, cDNA from leaves treated with only NOS cofactors and substrate.

different protein refolding protocols (Schein, 1989). Therefore, we were unable to test its sensitivity to NO. The low activity of the recombinant protein could be due to improper expression in *E. coli* or to the previously described recalcitrance of plant aconitases to reactivation.

Size heterogeneity occurs among the aconitase family, with sizes reported ranging from 86 kD for *Saccharomyces cerevisiae* to 120 kD for the *Bacillus subtilis* aconitase (De Bellis et al., 1993). Based on the sequence of the cytosolic aconitase, the predicted molecular mass is 98 kD; however, SDS-PAGE analysis shows an apparent size of approximately 108 kD for tobacco aconitase partially purified from leaves (Fig. 2). The anomalous migration of tobacco aconitase in SDS-PAGE was probably not due to glycosylation, because the *E. coli*-expressed recombinant protein also gives a larger than predicted size by SDS-PAGE.

Expression of Aconitase mRNA

Expression of the tobacco aconitase gene was first examined by northern-blot analysis using the *NtACO1* cDNA as a probe. Expression was not readily detected by northern analysis, suggesting that the cytosolic aconitase mRNA was present in low abundance (data not shown). Previous studies have shown that the aconitase mRNA is of low abundance in Arabidopsis (Peyret et al., 1995). Steady-state levels of aconitase mRNA are also low in animals, leading to the use of RT-PCR for mRNA analyses (Gosiewska et al., 1996). Therefore, RT-PCR with primers based on the *NtACO1* sequence was used to examine aconitase expression in various tobacco tissues and in response to NO treatment, as shown in Figure 5.

Expression of *NtACO1* was higher in flowers (lane 2) than in leaves (lane 1), as was also reported in Arabidopsis (Peyret et al., 1995). Furthermore, expression in tobacco flowers was not restricted to a specific floral part, as *NtACO1* levels were high in the various flower tissues examined, including petals (lane 4), anthers (lane 5), and ovaries (lane 6). In addition, mature flowers seemed to have slightly higher levels than those found in buds (lane 3). Expression of *NtACO1* did not change in leaves infiltrated with recombinant NOS (Fig. 5, lane 7) or after treatment for 3 to 24 h with various NO donors (SIN-1, SNAP, and GSNO; data not shown). Thus, NO does not appear to induce *NtACO1*. TMV infection, SA, or H_2O_2 treatment also did not induce *NtACO1* expression (data not shown).

DISCUSSION

For over a decade, NO has been known to function as an important signal molecule in animals; however, its role in plants is less well defined. Recently, NO was implicated as a signal for a variety of plant processes, including leaf expansion (Leshem, 1996) and root growth (Gouvea et al., 1997). In addition, NO signaling appears to be involved in activating defense responses to pathogens in potato, soybean, Arabidopsis, and tobacco (Noritake et al., 1996; Delledonne et al., 1998; Durner et al., 1998). As a step toward elucidating the mode(s) of NO action in plants, we sought to identify NO targets or effectors in tobacco. In this paper we demonstrate that aconitase is a NO target in tobacco and discuss possible ramifications of this inhibition.

Given the recent demonstration of NO synthesis during plant defense responses (Delledonne et al., 1998; Durner et al., 1998), the effect of NO on aconitase, a key NO and redox sensor in animals, is of considerable interest. Tobacco aconitases, like their mammalian counterparts, are inhibited by NO. Two different NO donors, SIN-1 and NOC-9, inhibited tobacco aconitase activity in vitro (Fig. 3). For example, a 15-min treatment with 1 mM NOC-9 caused a complete inhibition of partially purified aconitase activity. Aconitase was also extremely sensitive to H_2O_2, with 25 μM H_2O_2 inhibiting over 70% of activity (Fig. 3C). These results suggest that conditions leading to elevated levels of NO or other ROS will inactivate aconitase in tobacco.

ROS production during plant-pathogen interactions is well established and is believed to have important roles in activating various defense responses, including the hypersensitive response (HR), cell wall strengthening, and systemic acquired resistance (Mehdy et al., 1996; Alvarez and Lamb, 1997; Doke, 1997; Van Camp et al., 1998). Since both NO and other ROS are generated during defense responses to TMV and other pathogens, it is highly likely that aconitase is inactivated in cells undergoing an HR. Aconitase inactivation, in addition to disturbing mitochondrial energy metabolism, should result in elevated citrate concentrations. Increased citrate levels may serve as a defense strategy, since citrate is known to induce alternative oxidase (Vanlerberghe and McIntosh, 1996), which is implicated in resistance to TMV and other viruses (Chivasa and Carr, 1998; Murphy et al., 1999).

The inhibition of aconitase by NO may alter iron homeostasis in tobacco. NO would increase free iron levels if the NO-inactivated tobacco aconitase can act as an IRP. In animals, NO activation of the IRP results in elevated intracellular iron levels due to reduced translation of proteins that utilize or sequester iron (aminolevulinic acid synthase and ferritin, respectively) and increased stability of the mRNA for the transferrin receptor, which imports iron into the cell (Hentze and Kuhn, 1996). While the tobacco aconitase has not yet been shown to be a functional IRP, free iron levels may still increase due to the destruction of the

aconitase iron-sulfur cluster by NO and other ROS (Stamler, 1994; Rouault and Klausner, 1996). An increase in free iron could have a defensive function in tobacco following pathogen attack. Much of the oxidative damage in biological systems is mediated via iron through the Fenton reaction, in which H_2O_2 reacts with iron (Fe^{2+}) to yield the highly reactive hydroxy radical (Liochev, 1996; Rouault and Klausner, 1997). Interestingly, elevated levels of free iron resulting from destruction of the iron-sulfur clusters of aconitase and other dehydratases by NO or other ROS have been implicated in lipid peroxidation and DNA damage (Keyer and Imlay, 1996; Liochev and Fridovich, 1997). Thus, NO and other ROS could contribute to HR cell death in TMV-infected tobacco leaves by elevating free iron levels, by destabilizing iron-sulfur clusters, and/or perhaps by converting the tobacco cytoplasmic aconitase into a functional IRP. The presence of ROS plus elevated iron in cells undergoing a HR would likely create a killing environment for both host and pathogen. Additionally, while aconitase may be the most labile NO mitochondrial target, NO and other ROS can destroy the iron-sulfur clusters of other mitochondrial enzymes, which further increases levels of free iron (Kroncke et al., 1997).

As a first step to address whether tobacco contains a cytosolic isoform of aconitase that can be converted into an IRP in the presence of NO, a cDNA encoding a putative cytosolic aconitase was isolated. This cDNA, named *NtACO1*, has over 90% identity with a pumpkin cytosolic aconitase at the amino acid level (Hayashi et al., 1995). In addition, NtACO1 shares 76% amino acid sequence similarity with the human IRP-1 (Fig. 4). Moreover, NtACO1 contains the amino acid residues known to be important for mRNA binding by IRP-1. Thus, this protein may have the capacity to act as an mRNA-binding protein. However, preliminary attempts to detect IRP activity in plants have not been successful (Rothenberger et al., 1990; Hentze and Kuhn, 1996) and ferritin regulation may be different between plants and animals (Lescure et al., 1991). Bacteria were thought to not contain IRPs. However, the recent discovery that the *B. subtilis* aconitase binds rabbit ferritin IRE and IRE-like sequences in the *B. subtilis* operons that encode the major cytochrome oxidase and iron uptake system shows IRP activity is even more widespread than previously thought. This suggests that the tobacco cytosolic aconitase may also be an IRP. While plant aconitase has not yet been shown to influence gene expression by functioning as an mRNA-binding protein, aconitase has been demonstrated to influence gene expression in a plant-pathogen interaction. Wilson et al. (1998) showed that the *Xanthomonas campestris rpfA* gene, which regulates the production of pathogenicity factors, is an aconitase.

Using RT-PCR, the expression of *NtACO1* was monitored in various tissues, as well as in response to TMV infection or NO, SA, or H_2O_2 treatment. Aconitase mRNA was found to be expressed at a higher level in flowers than in leaves, as has been observed in Arabidopsis (Peyret et al., 1995). Aconitase mRNA expression was not induced by NO (Fig. 5), SA, or H_2O_2, a result consistent with the regulation of aconitase in animals, in which aconitase activity is primarily regulated post-translationally (Tang et al., 1992; Henderson and Kuhn, 1995). In this post-translational regulation, the iron-sulfur cluster is turned over much faster than the protein itself, thus enabling aconitase to serve as an iron sensor in which the cluster may be reassembled when sufficient iron and sulfur are present (Rouault and Klausner, 1997).

Similarities between NO signaling in plants and animals include increased production of NO during infection and possible roles for cGMP and cADP Rib as NO second messengers during defense responses (Delledonne et al., 1998; Durner et al., 1998). Furthermore, increases in NO levels are associated with viral disease resistance in both plants and animals (Durner et al., 1998; Reiss and Komatsu, 1998). NO is a major mediator of the vertebrate innate immune response with which plant defense mechanisms have substantial parallels. Similarities include the involvement of heterotrimeric G-proteins, phospholipases, NO generation, NADPH oxidase activation, and the synergism of NO and other ROS to kill pathogens. In addition, possible plant homologs of several animal proteins involved in disease resistance signaling pathways have been identified. For example, Arabidopsis NPR1 and the tobacco *N* gene have homology to the animal IκB product and *Drosophila* Toll and mammalian interleukin-1 receptor, respectively (Low and Dwyer, 1994; Baker et al., 1997; Cao, et al., 1997; Ryals et al., 1997; Yang et al., 1997; Scheel, 1998). The discovery that NO inhibits aconitase, suggests a variety of mechanisms through which NO might mediate disease resistance or other physiological processes. Thus, evidence continues to accumulate suggesting that NO may be a key signal molecule in plants and that NO signaling in plant defense responses has extensive parallels with animal NO signaling.

ACKNOWLEDGMENTS

We thank Dr. Pradeep Kachroo for his generous help and advice. We appreciate the efforts of Dr. D'Maris Dempsey in the critical reading of the manuscript.

Received August 9, 1999; accepted October 21, 1999.

LITERATURE CITED

Alen C, Sonenshein AL (1999) *Bacillus subtilis* aconitase is an RNA-binding protein. Proc Natl Acad Sci USA **96:** 10412–10417

Alvarez ME, Lamb C (1997) Oxidative burst-mediated defense responses in plant disease resistance. *In* JG Scandalios, ed, Oxidative Stress and the Molecular Biology of Antioxidant Defenses. Cold Spring Harbor Laboratory Press, Cold Spring Harbor, NY, pp 815–838

Baker B, Zambryski P, Staskawicz B, Dinesh-Kumar SP (1997) Signaling in plant-microbe interactions. Science **276:** 726–733

Basilion JP, Rouault TA, Massinople CM, Klausner RD, Burgess WH (1994) The iron-responsive element-binding protein: localization of the RNA-binding site to the aconitase active-site cleft. Proc Natl Acad Sci USA **91:** 574–578

Bouton C, Hirling H, Drapier JC (1997) Redox modulation of iron regulatory proteins by peroxynitrite. J Biol Chem **272:** 19969–19975

Brouquisse R, Nishimura M, Gaillard J, Douce R (1987) Characterization of a cytosolic aconitase in higher plant cells. Plant Physiol **84:** 1402–1407

Cao H, Glazebrook J, Clark JD, Volko S, Dong X (1997) The Arabidopsis NPR1 gene that controls systemic acquired resistance encodes a novel protein containing ankyrin repeats. Cell **88:** 57–63

Castro L, Rodriguez M, Radi R (1994) Aconitase is readily inactivated by peroxynitrite, but not by its precursor, nitric oxide. J Biol Chem **269:** 29409–29415

Chivasa S, Carr JP (1998) Cyanide restores N gene-mediated resistance to tobacco mosaic virus in transgenic tobacco expressing salicylic acid hydroxylase. Plant Cell **10:** 1489–1498

Courtois-Verniquet F, Douce R (1993) Lack of aconitase in glyoxysomes and peroxisomes. Biochem J **294:** 103–107

De Bellis L, Hayashi M, Nishimura M, Alpi A (1995) Subcellular and developmental changes in distribution of aconitase isoforms in pumpkin cotyledons. Planta **195:** 464–468

De Bellis L, Tsugeki R, Alpi A, Nishimura M (1993) Purification and characterization of aconitase isoforms from etiolated pumpkin cotyledons. Physiol Plant **88:** 485–492

Delledonne M, Xia Y, Dixon RA, Lamb C (1998) Nitric oxide functions as a signal in plant disease resistance. Nature **394:** 585–588

Doke N (1997) The oxidative burst: roles in signal transduction and plant stress. *In* JG Scandalios, ed, Oxidative Stress and the Molecular Biology of Antioxidant Defenses. Cold Spring Harbor Laboratory Press, Cold Spring Harbor, NY, pp 785–813

Domachowske JB (1997) The role of nitric oxide in the regulation of cellular iron metabolism. Biochem Mol Med **60:** 1–7

Drapier JC (1997) Interplay between NO and [Fe-S] clusters: relevance to biological systems. Comp Methods Enzymol **11:** 319–329

Durner J, Wendehenne D, Klessig DF (1998) Defense gene induction in tobacco by nitric oxide, cyclic GMP and cyclic ADP ribose. Proc Natl Acad Sci USA **95:** 10328–10333

Fukuto JM (1995) Chemistry of nitric oxide: biologically relevant aspects. Adv Pharmacol **34:** 1–15

Gardner PR, Costantino G, Szabo C, Salzman AL (1997) Nitric oxide sensitivity of the aconitases. J Biol Chem **272:** 25071–25076

Gardner PR, Fridovich I (1991) Superoxide sensitivity of the *Escherichia coli* aconitase. J Biol Chem **266:** 19328–19333

Gardner PR, Raineri I, Epstein LB, White CW (1995) Superoxide radical and iron modulate aconitase activity in mammalian cells. J Biol Chem **270:** 13399–13405

Gosiewska A, Mahmoodian F, Peterkofsky B (1996) Gene expression of iron-related proteins during iron deficiency caused by scurvy in guinea pigs. Arch Biochem Biophys **325:** 295–303

Gouvea CMCP, Souza JF, Magalhaes ACN, Martins IS (1997) NO-releasing substances that induce growth elongation in maize root segments. Plant Growth Reg **21:** 183–187

Grune T, Blasig IE, Sitte N, Roloff B, Haseloff R, Davies KJ (1998) Peroxynitrite increases the degradation of aconitase and other cellular proteins by proteasomes. J Biol Chem **273:** 10857–10862

Guo A, Durner J, Klessig DF (1998) Characterization of a tobacco epoxide hydrolase gene induced during the resistance response to TMV. Plant J **15:** 647–656

Hausladen A, Stamler JS (1998) Nitric oxide in plant immunity. Proc Natl Acad Sci USA **95:** 10345–10347

Hayashi M, De Bellis L, Alpi A, Nishimura M (1995) Cytosolic aconitase participates in the glyoxylate cycle in etiolated pumpkin cotyledons. Plant Cell Physiol **36:** 669–680

Henderson BR, Kuhn LC (1995) Differential modulation of the RNA-binding proteins IRP-1 and IRP-2 in response to iron: IRP-2 inactivation requires translation of another protein. J Biol Chem **270:** 20509–20515

Hentze MW, Kuhn LC (1996) Molecular control of vertebrate iron metabolism: mRNA-based regulatory circuits operated by iron, nitric oxide, and oxidative stress. Proc Natl Acad Sci USA **93:** 8175–8182

Hill RL, Bradshaw RA (1969) Fumarase. Methods Enzymol **13:** 91–99

Ischiropoulos H (1998) Biological tyrosine nitration: a pathophysiological function of nitric oxide and reactive oxygen species. Arch Biochem Biophys **356:** 1–11

Kaptain S, Downey WE, Tang C, Philpott C, Haile D, Orloff DG, Harford JB, Rouault TA, Klausner RD (1991) A regulated RNA binding protein also possesses aconitase activity. Proc Natl Acad Sci USA **88:** 10109–10113

Kennedy MC, Emptage MH, Dreyer JL, Beinert H (1983) The role of iron in the activation-inactivation of aconitase. J Biol Chem **258:** 11098–11105

Keyer K, Imlay JA (1996) Superoxide accelerates DNA damage by elevating free-iron levels. Proc Natl Acad Sci USA **93:** 13635–13640

Klausner RD, Rouault TA, Harford, JB (1993) Regulating the fate of mRNA: the control of cellular iron metabolism. Cell **72:** 19–28

Kroncke KD, Fehsel K, Kolb-Bachofen V (1997) Nitric oxide: cytotoxicity versus cytoprotection: how, why, when, and where? Nitric Oxide Biol Chem **1:** 107–120

Lancaster JR (1997) A tutorial on the diffusibility and reactivity of free nitric oxide. Nitric Oxide Biol Chem **1:** 18–30

Lescure AM, Proudhon D, Pesey H, Ragland M, Theil EC, Briat JF (1991) Ferritin gene transcription is regulated by iron in soybean cell cultures. Proc Natl Acad Sci USA 88: 8222–8226

Leshem YY (1996) Nitric oxide in biological systems. Plant Growth Reg **18:** 155–159

Liochev SI (1996) The role of iron-sulfur clusters in *in vivo* hydroxy radical production. Nitric Oxide Biol Chem **25:** 369–384

Liochev SI, Fridovich I (1997) How does superoxide dismutase protect against tumor necrosis factor: a hypothesis informed by effect of superoxide on "free" iron. Nitric Oxide Biol Chem **23:** 668–671

Low PS, Dwyer SC (1994) Comparison of the oxidative burst signaling pathways of plants and human neutrophils. Adv Mol Genet Plant-Microbe Int **3:** 361–369

Malamy J, Hennig J, Klessig DF (1992) Temperature-dependent induction of salicyclic acid and its conjugates during the resistance response to tobacco mosaic virus infection. Plant Cell **4:** 359–365

Mehdy MC, Sharma YK, Sathasivan K, Bays NW (1996) The role of activated oxygen species in plant disease resistance. Physiol Plant **98:** 365–374

Melino G, Bernassola F, Knight RA, Corasaniti MT, Nistico G, Finazzi-Agro A (1997) S-Nitrosylation regulates apoptosis. Nature **388:** 432–433

Mott HR, Carpenter JW, Campbell SL (1997) Structural and functional analysis of a mutant Ras protein that is insensitive to nitric oxide activation. Biochemistry **36:** 3640–3644

Murphy AM, Chivasa S, Singh DP, Carr JP (1999) Salicyclic acid-induced resistance to viruses and other pathogens: a parting of the ways? Trends Plant Sci **4:** 155–160

Nathan C (1995) Natural resistance and nitric oxide. Cell **82:** 873–876

Noritake T, Kawakita K, Doke N (1996) Nitric oxide induces phytoalexin accumulation in potato tuber tissues. Plant Cell Physiol **37:** 113–116

Pantopoulos K, Hentze MW (1995) Rapid responses to oxidative stress mediated by iron regulatory protein. EMBO J **14:** 2917–2924

Peyret P, Perez P, Alric M (1995) Structure, genomic organization and expression of the *Arabidopsis thaliana* aconitase gene. J Biol Chem **270:** 8131–8137

Philpott CC, Klausner RD, Rouault TA (1994) The bifunctional iron-responsive element binding protein/cytosolic aconitase: the role of active-site residues in ligand binding and regulation. Proc Natl Acad Sci USA **91:** 7321–7325

Reiss CS, Komatsu T (1998) Does nitric oxide play a critical role in viral infections? J Virol **72:** 4547–4551

Rothenberger S, Mullner EW, Kuhn LC (1990) The mRNA-binding protein which controls ferritin and transferrin receptor expression is conserved during evolution. Nucleic Acids Res **18:** 1175–1179

Rouault T, Klausner R (1997) Regulation of iron metabolism in eukaryotes. Curr Top Cell Regul **35:** 1–19

Rouault TA, Klausner RD (1996) Iron-sulfur clusters as biosensors of oxidants and iron. Trends Biochem Sci **21:** 174–177

Ryals J, Weymann K, Lawton K, Friedrich L, Ellis D, Steiner HY, Johnson J, Delaney TP, Jesse T, Vos P, Uknes S (1997) The Arabidopsis NIM1 protein shows homology to the mammalian transcription factor inhibitor I kappa B. Plant Cell **9:** 425–439

Sambrook, Fritsch E, Maniatis T (1989) Molecular Cloning: A Laboratory Manual, Ed 2. Cold Spring Harbor Laboratory Press, Cold Spring Harbor, NY

Scheel D (1998) Resistance response physiology and signal transduction. Curr Opin Plant Biol **1:** 305–310

Schein C (1989) Production of soluble recombinant proteins in bacteria. Biotechnology **7:** 1141–1148

Schmidt HHWH, Walter U (1994) NO at work. Cell **78:** 919–925

Stamler JS (1994) Redox signaling: nitrosylation and related target interactions of nitric oxide. Cell **78:** 931–936

Tang CK, Chin J, Harford JB, Klausner RD, Rouault TA (1992) Iron regulates the activity of the iron-responsive element binding protein without changing its rate of synthesis or degradation. J Biol Chem **267:** 24466–24470

Van Camp W, Montagu MV, Inzé D (1998) H_2O_2 and NO: redox signals in disease resistance. Trends Plant Sci **3:** 330–334

Vanlerberghe GC, McIntosh L (1996) Signals regulating the expression of the nuclear gene encoding alternative oxidase of plant mitochondria. Plant Physiol **111:** 589–595

Verniquet F, Gaillard J, Neuburger M, Douce R (1991) Rapid inactivation of plant aconitase by hydrogen peroxide. Biochem J **276:** 643–648

Wilson TJ, Bertrand N, Tang JL, Feng JX, Pan MQ, Barber CE, Dow JM, Daniels MJ (1998) The rpfA gene of *Xanthomonas campestris* pathovar *campestris*, which is involved in the regulation of pathogenicity factor production, encodes an aconitase. Mol Microbiol **28:** 961–970

Yan LJ, Levine RL, Sohal RS (1997) Oxidative damage during aging targets mitochondrial aconitase. Proc Natl Acad Sci USA **94:** 11168–11172

Yang Y, Shah J, Klessig DF (1997) Signal perception and transduction in plant defense responses. Genes Dev **11:** 1621–1639